nature reviews materials

https://doi.org/10.1038/s41578-023-00581-x

Review article

Check for updates

New opportunities and old challenges in the clinical translation of nanotheranostics

In the format provided by the authors and unedited

Supplementary Information

NEW OPPORTUNITIES AND OLD CHALLENGES IN THE CLINICAL TRANSLATION OF NANOTHERANOSTICS

Peter J. Gawne[1,2,3], Miguel Ferreira[4], Marisa Papaluca[5], Jan Grimm[6] & Paolo Decuzzi[7♠]

[1] UCL Cancer Institute, University College London, London, UK.

[2] Centre for Cancer Biomarkers and Biotherapeutics, Barts Cancer Institute, Queen Mary, University of London, London, UK.

[3] School of Biomedical Engineering and Imaging Sciences, King's College London, London, UK.

[4] Department of Radiology, Harvard Medical School, Massachusetts General Hospital, Boston, MA, USA

[5] School of Public Health, Imperial College of London, South Kensington Campus London, UK

[6] Molecular Pharmacology Program and Department of Radiology, Memorial Sloan-Kettering Cancer Center, New York, NY, USA

[7] Laboratory of Nanotechnology for Precision Medicine, Fondazione Istituto Italiano di Tecnologia, Via Morego 30, 16163, Genoa, IT

♠ Corresponding author: Paolo Decuzzi, PhD; paolo.decuzzi@iit.it

The authors contributed equally to all aspects of the article.

1 PRECLINICAL NANOTHERANOSTICS

A simple bibliographic search for 'theranostic' AND 'nanoparticles' in Scopus returns almost 6,000 scientific manuscripts published over the course of 10 years, steadily growing from about 2 manuscripts per week in 2012 to 3 manuscripts per day in 2021 (**Supplementary Figure 1**). Among the different imaging modalities, Magnetic Resonance and Radionuclide imaging cover 70% of all the publications, with a slight preference for the former over the latter, followed by optical imaging and ultrasound with about 20% and 10% of the manuscripts, respectively. Multiple manuscripts describe hybrid systems where two and more imaging modalities are integrated together. The level of diversity increases dramatically when the therapeutic modality and nanocarrier compositions are taken into the picture. For theranostic nanoparticles in preclinical development, photothermal therapy (PTT), chemotherapy, and photodynamic therapy (PDT) appear to be the most common therapeutic modalities. In terms of material composition, gold and iron oxide dominates over silica, lipids, and polymers, mostly because of their intrinsic imaging and therapeutic properties.

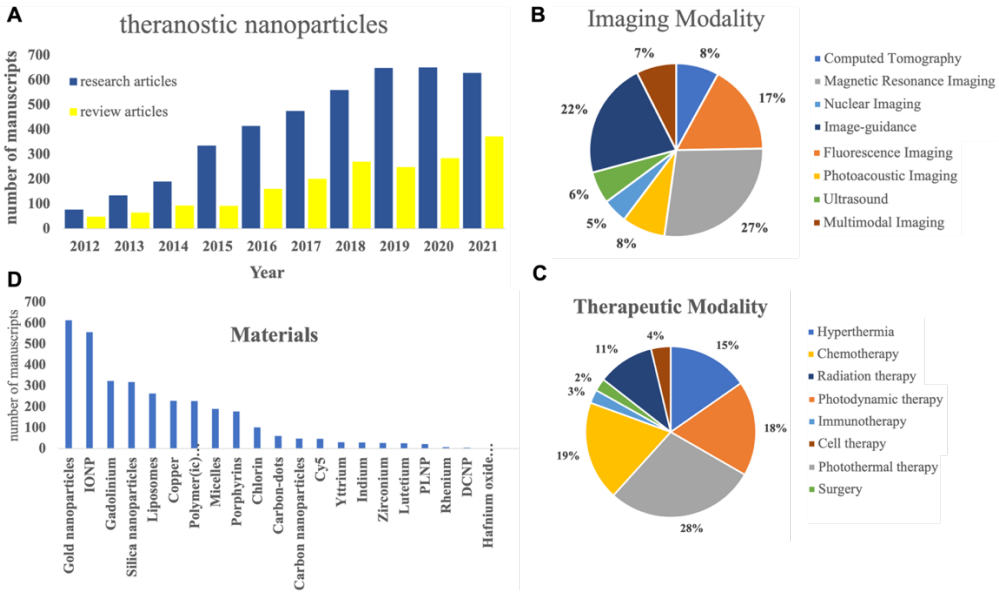

Supplementary Figure 1. Analysis of the scientific publications related to theranostic nanoparticles. A. Number of publications citing 'theranostic' AND 'nanoparticles' in the Abstract, Title, and Keywords as extracted from Scopus between 2012 and 2021. The blue bars are related to research articles, whereas the yellow bars correspond to review papers. **B.**

Primarily used Imaging Modalities for the research articles published in the period 2012 – 2021. Data are extracted from Scopus searching for the name of the imaging modality in the Abstract, Title, and Keywords. **C.** Primarily used Therapeutic Modalities for the research articles published in the period 2012 – 2021. Data are extracted from Scopus searching for the name of the therapeutic modality in the Abstract, Title, and Keywords. **D.** Primarily cited Materials used for realizing the nanocarriers in the research articles published in the period 2012 – 2021. Data are extracted from Scopus searching for the material name in the Abstract, Title, and Keywords.

1.1 Magnetic Resonance Imaging and Nanomedicines

Magnetic Resonance Imaging (MRI) is an imaging technique providing high spatial resolution without depth limitations or the use of ionizing radiation. The primary nuclei used for MRI contrast are protons (^{1}H), which are one of the most abundant nuclei in body tissues. Anatomical imaging contrast in MRI is generated by the different longitudinal (T_1) and transverse (T_2) relaxation times of protons present in different tissues, after their excitation by an RF pulse. Whilst the soft tissue contrast of MRI is outstanding, the signal-to-background ratio of MRI is meager due to the high abundance of protons resulting in overall low sensitivity.[1] This limitation can be mitigated by use of exogenous imaging agents to enhance T_1 and T_2 contrast in tissues.[2] Hence, MRI-based nanotheranostics frequently combine an exogenous contrast agent with a therapeutic payload into a single nanocarrier, often functionalized with a targeting moiety.[3-5] One prominent example of encapsulated nanotheranostics reported the incorporation of gadolinium diethylenetriamine pentaacetic acid (Gd-DTPA) for T_1 MRI contrast and platinum drug molecules as a therapeutic agent into the core of polymeric micelles.[6] *In vivo* MR imaging successfully correlated high tumor contrast enhancement with high rates of tumor mass shrinkage. Activatable MRI nanotheranostic particles have been engineered to release the drug after a trigger from an endogenous signal, e.g., changes in pH and redox environments. This allows the exploitation of the acidic tumor microenvironment to trigger drug release from nanotheranostics with ionizable or acid-sensitive components [7] [8]. A key example utilized poly(acrylic acid) (PAA)-coated iron oxide nanoparticles conjugated with an $\alpha_v\beta_3$ integrins, targeting the RGD peptides, and doxorubicin (DOX) using pH-responsive poly(ethylene glycol)methyl ether (mPEG) chains, as schematically depicted in **Figure 2A**. At acidic pH only, the hydrolysis of the PEG polymer exposed the RGD ligand allowing integrin-specific binding [9]. Treatment of U87MG tumor-bearing mice showed high tumor

accumulation and high therapeutic efficacy; with partial or complete regression of tumors due to combined passive and active tumor targeting and pH-responsive release of doxorubicin molecules. This is a clear example of a hybrid nanotheranostics combining doxorubicin encapsulation with the innate MR imaging contrast enhancement of the iron oxide nanoparticles. Redox active MRI-nanotheranostics have also been designed allowing selective therapeutic cargo release in tumors.[10] An example of this strategy used glutathione (GSH)-responsive CaO_2 nanoparticles loaded with MnO_2 and DOX, and stealth-coated with 4T1 cancer cell membranes. Tumor cells with high levels of GSH trigger the release of DOX for tumor therapy and release of Mn^{2+} thus enhancing T_1 relaxivity [11]. Additionally, the CaO_2 core amplifies the tumor's oxidative stress *via* the generation of H_2O_2 and Ca^{2+} to kill cancer cells more efficiently, leading to 4T1 tumor growth suppression in murine models.

1.2 Magnetic Resonance Imaging and Thermal Ablation

Along with agents designed to respond to endogenous stimuli, whose efficacy could be limited by the biological heterogeneity of the local environment [12], nanotheranostics can also be activated using exogenously applied triggers; for example combining localized heating and MR imaging. This is the case of superparamagnetic iron oxide (SPIO) nanoparticles. These are sufficiently small (< 30 nm) iron oxide based particles that could be simultaneously used as potent T_2 MR imaging contrast agents and heat generators, upon stimulation via external alternating magnetic fields creating local particle vibrations and thus heat generation from friction, as schematically depicted in **Figure 2B**.[13] Depending on the particle concentration and their physico-chemical properties, the features of the externally applied magnetic field and of the biological tissue, SPIO can heat tissue up to 42 – 45°C (hyperthermia) or even above 60°C (thermal ablation). In a recent example, nanotheranostic particles were prepared using dextran-coated Fe_3O_4 nanoparticles conjugated with folic acid.[14] T_2-weighted MRI was used to demonstrate particle deposition within the tumor. Multiple dosing cycles with the application of an external magnetic field resulted in a significant reduction in tumor progression. Cho and collaborators engineered clusters of 20 nm iron oxide nanocubes to boost the transverse relaxivities and heating efficiency [15]. In a more recent study, 18 nm theranostic magnetic ferrite nanoparticles have been demonstrated for dual-mode Magnetic Resonance / Magnetic Particle imaging (MRI/MPI) and magnetic hyperthermia in 4T1 orthotopic mouse breast cancer models [16]. Also, the groups of Pellegrino and Gazeau have engineered

magnetic thermoresponsive iron oxide nanocubes to combine heat-mediated drug delivery with magnetic hyperthermia and MR imaging [17].

As an alternative to magnetic field, thermal ablation can be also obtained through the near-infrared (NIR) excitation of photothermal agents (PTAs). Upon light absorption, the PTA converts the light energy into heat, inducing local hyperthermia in a process known as photothermal therapy (PTT). Therefore, it causes tumor tissue ablation through thermal damage [18]. PTAs have the ability to generate local temperatures over 50 °C. Due to its high spatial resolution, MRI can be used to accurately delineate the tumor site for PTT, guiding the application of the laser beam for PTT and reducing possible damage to the healthy tissue.

1.3 Magnetic Resonance Imaging and Radiation therapy

Radiosensitizing nanoparticles are also being investigated to overcome resistance in radiotherapy, due to tumor hypoxia and dose constraints to prevent damaging the normal tissue [19]. MRI nanotheranostics have been tested as radiosensitisers themselves or as carriers of radiosensitizing agents. This is often achieved by integrating into the nanocarrier structure heavy metals (e.g., Au, Bi, Gd), which exhibit high X-ray photon capture cross-section and Compton scattering effect, as schematically shown in **Figure 2C**.[20] One key example used hyaluronic acid-functionalized Gd_2O_3 nanoparticles for magnetic resonance imaging-guided radiotherapy of tumors.[21] The gadolinium-based nanoparticles were decorated with hyaluronic acid (HA) chains that provided the targeting potential and helped boosting the longitudinal relaxivity. In HepS tumor-bearing mice, a synergistic effect was obtained using these nanoparticles along with radiotherapy, with the MR imaging preformed to monitor particle uptake. This is an example of innate nanotheranostics where the Gd_2O_3 nanoparticles function simultaneously as enhancers of the MR imaging contrast and external beam radiation therapy.

1.4 MRI-guided HIFU triggering of nanomedicines

The High Intensity Focused Ultrasound (HIFU) therapy relies on the localized absorption of acoustic energy and its transformation in heat with the objective of ablating the diseased cells. While low ultrasound frequencies (< 20 kHz) can be used for imaging purposes, high frequencies (> 20 kHz) are strong enough to induce the release of a therapeutic payload, enhance the permeability of the cell membrane as well as tissue.[22] As an example, MRI combined with HIFU

has been proposed as a curative strategy for musculoskeletal tumors, which is a very promising application given the high acoustic absorption of bone [23].

In addition to this, MRI and HIFU can be used together with nanoparticles leading to complex nanotheranostic systems (**Figure 2D**). A prominent example reports liposomes encapsulating combretastatin A4 phosphate (CA4P), a vascular disrupting agent, and magnetic maghemite (γ-Fe_2O_3) nanoparticles. Liposomes were formulated with lipids exhibiting a transition temperature around 43 °C, which was readily overcome upon local HIFU stimulation thus triggering drug release. In the same liposomes, the maghemite nanoparticles provided T_2-weighted MR imaging capability as well as the magnetic targeting of the tumor tissue.[24] Administration of the CA4P-containing liposomes along with magnetic targeting and HIFU demonstrated significant tumor growth suppression. Additionally, as well as increasing local drug release, hyperthermia using HIFU can also increase tumor permeability leading to increased nanotheranostic uptake. For example, nanotheranostic liposomes containing the anticancer agent topotecan, a topoisomerase 1 inhibitor – along with lipids conjugated with Gd and a NIR dye – were used in combination with repeated FUS treatments leading to higher tumor accumulation validated using both MRI or NIRF.[25]

1.5 Radionuclide Imaging and Nanomedicines

Radionuclide imaging – positron emission tomography (PET) or single photon emission computed tomography (SPECT) – allows quantitative imaging on the whole-body scale without depth limitations. In particular, the sensitivity and quantitative nature of PET easily allows elucidation of whole-body pharmacokinetics, biodistribution and target accumulation of different radiolabeled nanomaterials, as schematically depicted in **Figure 2E**. [26] This can be highly valuable for validating new nanomedicine formulations to aid clinical translation.[27] For example, PET imaging was used to screen a library of lipoprotein-based nanoparticles, with varying sizes, shapes and composition, as candidates for atherosclerosis treatment.[28] After radiolabeling with ^{89}Zr, their in vivo behavior was then evaluated with PET imaging allowing a quantitative comparison of their pharmacokinetics and aortic uptake in murine models of atherosclerosis. The specific properties of PET imaging also make it applicable to various scales, from small animals to humans – most recently with rapid whole-body imaging scanning [29]. For example, simvastatin-loaded high-density lipoprotein nano-immuno-therapeutics radiolabeled with ^{89}Zr allowed for quantitative in

vivo imaging in large animal models of atherosclerosis (porcine and rabbits) on the whole-body scale [30].

Another key role that PET imaging may allow is the assessment of target accumulation in patients undergoing treatment with nanomedicines, particularly for formulations whose accumulation is predominantly driven by the enhanced permeability and retention (EPR) effect.[31-33] By imaging nanomedicines non-invasively within patients, they can be grouped into potential responders and non-responders allowing treatment stratification – a concept aiming to establish *personalized nanomedicine*.[34] To implement this, the radiolabeling of nanomedicines without substantially affecting their physio-chemical properties is necessary.[35 36] Alternatively, a potentially more robust nanotheranostic method would be to deploy a 'companion diagnostic'[37] or PET nanoreporter[38], which demonstrates similar EPR-mediated uptake. This was documented in two independent studies using radiolabeled liposomes that could be injected both prior-to or with the nanomedicines – allowing prediction of therapeutic response in preclinical cancer models. Each study was able to demonstrate good correlation between the PET signal and the amount of drug deposited at the tumor site. In particular, Reiner and colleagues have developed ^{89}Zr-labeled liposomes to possibly screen cancer patients for the accumulation of the liposomal nanomedicine Doxil.[38] A pegylated liposome was labelled with ^{89}Zr using the chelating agent desferrioxamine B. This resulted in ^{89}Zr-liposomes with a characteristic diameter of ~ 110 nm and a surface ζ-potential of -26 mV versus Doxil presenting a diameter of ~ 85 nm and a surface ζ-potential of -31 mV. These apparently minor differences could be the reason for significant differences in the pharmacokinetics profiles of the two particles. Nonetheless, a clear correlation was observed between the intratumor deposition of doxorubicin, released from Doxil, and the radioactive signal associated with the ^{89}Zr accumulation. This approach has been further elaborate for in-human applications, as detailed in the following chapter.

1.6 Radionuclide Imaging and Radiation therapy

Along with imaging radionuclides, nanomaterials can also be labelled with therapeutic radionuclides emitting β^-- or α-particles upon decay. In the context of nanotheranostics, particles can be designed to integrate two different radionuclides: one to allow PET imaging of target accumulation and one for radiotherapy (**Figure 2F**). Crucially, the imaging and the therapeutic

agent must exhibit very similar pharmacokinetics; hence the two radionuclides should ideally have similar decay half-lives and coordination chemistry – a concept known as a 'theranostic pair' [39]. In one relevant study, polymeric nanostars were functionalized either with ^{89}Zr for in vivo quantification via PET imaging or with the beta-emitting ^{177}Lu for endo-radiotherapy. The nanostar tumor accumulation was compared between 'high EPR' (CT26 colon cancer isografts) and 'low EPR' (BxPC3 pancreatic cancer xenografts) tumor models, with significantly higher uptake observed in the former. Subsequent therapeutic studies using ^{177}Lu-nanostars demonstrated a dose-dependent decrease in tumor size and increase in cumulative survival in the 'high EPR' models. Indeed, this methodology could be implemented clinically using PET imaging to assess lesion uptake of the nanotheranostic before following up with radiotherapy. This procedure can be further simplified by removing the need for distinct chemical modifications and radiochemistry for imaging and radiotherapy. A recent example radiolabeled ultrasmall silica nanoparticles with the isotopic theranostic pair ^{86}Y/^{90}Y, which could be used for PET imaging (^{86}Y) or β^- radiotherapy (^{90}Y) respectively with a single chemically identical platform [40]. Imaging showed high uptake (10 % ID/g) of the ^{86}Y-nanoparticles in 4T1 tumors with a significant increase in survival observed in mice injected with the beta-emitting ^{90}Y-nanoparticles.

Besides standard radiotherapy applications, a more recent nanotheranostic strategy utilizes radionuclides to induce a photodynamic therapy (PDT) response. This method leverages the UV-blue light Cerenkov radiation (CR) generated by radionuclide decay to interact with a photosensitive nanomaterial triggering the emission of long-wavelength photons that produce cytotoxic reactive oxygen species (ROS), as pictured in **Figure 2G**. This strategy, known as Cerenkov radiation-induced therapy (CRIT), completely circumvents the need for external light sources; a major drawback for standard PDT – due to the limited tissue penetration of light. In the first major example, the systemic injection of titanium dioxide nanophotosensitisers decorated with tumor-targeting apo-transferrin (TiO_2-Tf) along with [^{18}F]FDG showed marked reduction in tumor growth.[41] This platform was expanded upon by directly radiolabeling the TiO_2-Tf nanophotosensitiser with ^{89}Zr leading to a nanotheranostic platform inherently capable of CRIT and PET imaging.[42] CRIT-based nanotheranostics of various compositions containing PDT-active chlorins [43] and porphyrins [44] have been reported subsequently. In a notable example, the amplification of CRIT was demonstrated by the pre-injection of a high dose of non-radioactive

PDT agent, followed by a low-dose of the radioactive CR-emitting nanocomplex. Porphyrin-PEG nanocomplexes capable of chelating ^{89}Zr (Df-PPN) were prepared and injected into 4T1-tumour bearing mice, followed by the ^{89}Zr-Df-PPN to 'detonate' the PDT nanocomplex via CRIT.[45] This combination resulted in significant tumor growth inhibition. Note that these are all examples of hybrid nanotheranostics where the innate properties of the nanophotosensitizers are combined with chelated radioactive metals.

1.7 Optical imaging and Phototherapies

Optical imaging utilizes photons emitted from bioluminescent or fluorescent probes for imaging acquisition (**Figure 2H**). It is a low-cost technique providing good spatial resolution over a wide spectrum, from visible to near-infrared (NIR) light, but it is limited by poor penetration, autofluorescence, and scattering of photons in the visible part of the spectrum (395 – 600 nm).[46, 47] Optical imaging agents can often be combined with photodynamic therapy (PDT) agents to form optical nanotheranostics. However, these agents can still be limited by issues of depth penetration of the local external irradiation – which inevitably damages normal tissue by overheating.[48]

This limitation can be partly overcome by using persistent luminescence nanoparticles (PLNP), which consist of three essential components: a host, an emitter, and a trap. The host is the carrier' backbone, as physico-chemical properties can influence the emitter's spectral structure. The emitter defines the luminescent wavelength of PLNP and is constituted by various metal ions. Finally, the trap is the energy state that can trap electrons in the forbidden band, usually formed by intrinsic defects or ion doping into the host. [49] Importantly, in vivo PLNP imaging of tumors can be obtained through different excitation sources, including UV,[50] LED,[51] NIR laser,[52, 53] X-ray,[54] and radiopharmaceutical.[55] In one key example of PLNP-based nanotheranostics, liposomes co-loaded with PLNP and paclitaxel dramatically inhibited tumor growth in MCF-7 tumor-bearing athymic mice.[56] Histology results demonstrated that the absence of damage to major organs, which was likely due to the fast hepatobiliary excretion of these particles. NIR PLNP can be reactivated using NIR light capable of deep tissue penetration, removing the need for continuous in situ excitation. One key example reported PDT-active NIR-emitting ultra-small PLNPs.[57] Brominated asymmetric cyanine (BAC) conjugated to PLNP allowed intersystem crossing from the lowest excited singlet (S1) state to the lowest excited triplet (T1) state, increasing the generation of

ROS.[58, 59] In vivo imaging and PDT studies demonstrated potent HeLa tumor suppression in mice, with the highest luminescent nanoparticle signal at 12h post injection. The therapeutic experiment resulted in complete tumor suppression when treated with continuous or fractionated laser exposure.

1.8 Optical imaging and Surgical therapy

A key application of nanoparticles for optical imaging is their use in fluorescence-guided surgery (FGS) for the resection of malignant masses. Complete resection of tumors can be at times challenging and depends on the visual localization of the tumor by the surgeon. Several studies show that residual tumor cells are associated with an increased local reoccurrence of the tumor [60]. FGS utilizes molecular imaging agents to detect tumor margins with high contrast, sensitivity, and sensitivity (**Figure 2I**) – whilst benefitting from low cost, safety and ease of use.[61] The use of nanoparticle-based molecular imaging agents with FGS has also been extensively explored, and can arguably be referred to as a nanotheranostic system. A key example used NIR-imageable lanthanide-based down-conversion nanoparticles (DCNP) modified with DNA and targeting peptides (NIR-DCNP) allowed the precise tumor resection in mice bearing subcutaneous $CaOV_3$ cells.[62] Additionally, the NIR-DCNP were capable to identify the boundaries of large tumors as well as small metastatic lesions. in mice bearing human ovarian adenocarcinoma peritoneal metastases.

Upon initial cancer diagnosis, staging becomes essential for any further therapy planning. Sentinel lymph nodes (SLN) are the first draining lymph nodes and the ones most likely to harbor cancer cells. This has motivated the use of imaging techniques to study SLN. In this case, the contrast agent is injected into the primary tumor and transported by the lymphatic system to the nearest SLN. Upon being internalized by macrophages, the contrast agents stay in the SLN. This allows for imaging and assists the SLN biopsy by helping to understand the number, location, and distribution.[63, 64] Small dye molecules, such as, methylene blue (MB), isosulfan blue (IB), and patent blue (PB) have been used for SNL imaging. However, they are cleared rapidly from the lymph nodes.[65-67] This led to the development of fluorescence imaging with emissive nanoparticles, which can achieve a higher signal-to-noise ratio, enhance the difference between lymph nodes from blood and other tissues. Additionally, nanotheranostics have been developed

for imaging of SLN and photothermal therapy of SLN metastasis. A key example utilized a fluorescent CuS nanoparticle labeled with a cRGD targeting agent and the NIR Cy5.5 dye for treating gastric cancer metastasis in SLNs.[68] In vivo studies in mice bearing MKN45 tumors showed that the nanoparticles were easily drained into SLN and capable of targeting the metastatic tumor cells and – when combined with PTT – resulted in their significantly reduced size and weight. However, there can be more than one draining SLN region and SLN identification can be false negative particularly when the nodes are already metastatic.[69, 70]

1.9 Photoacoustic Imaging and Nanotheranostics

Photoacoustic imaging (PAI) uses a pulse laser to irradiate light-absorbing molecules that, in turn, produce thermal expansion that generate pressure changes resulting in detectable ultrasonic waves (**Figure 2J**). In contrast with optical imaging, PAI can reach imaging depth of a few centimeters. Also, PAI can be used as a complementary imaging modality with other imaging techniques, such as US and optical imaging. PAI has been used in preclinical diagnosis for tumor, inflammation and infection monitoring, and metastatic lymph node detection [71]; using both endogenous agents (such as oxygenated-/deoxygenated-hemoglobin[72] or melanin[73] or exogenous agents (such as, gold nanostructures, carbon nanotubes, etc.) [74].

Within the context of nanotheranostics, PAI can be used to non-invasively observe drug release. In one interesting nanotheranostic study, indocyanine-conjugated mesoporous silica nanoparticles were loaded with a PAI-imageable, anticancer drug (mitoxantrone) in the nanoparticle core. Since both the indocyanine and mitoxantrone were detectable at different wavelengths with PAI, this allowed a multiplexed approach to non-invasively monitor drug delivery and release behavior from the nanoprobes[75]. An interesting example of this approach utilizes M1 macrophage-derived cellular nanovesicles (CNV) with tumor-homing and immune-reprogramming properties. CNV were loaded with gold nanorods (GNR), gemcitabine (GEM), cytosine-phosphate-guanine oligodeoxynucleotides, and a PD-L1 aptamer [76]. The local rapid hyperthermia and triggered release induced by NIR prevent side effects and limited the damage to healthy tissues. Furthermore, in vivo results showed complete remission of the tumor and survival until the end of the study for the group treated with CNV and NIR.

1.10 Focused Ultrasound and Enhanced Delivery

Ultrasound (US) is arguably one of the safest and most versatile imaging modalities. It is low-cost, provides excellent spatiotemporal resolution, and is widely used in the clinical setting whilst being limited to a small field of view and depth penetration. Focused ultrasound (FUS), in which the ultrasonic waves are focused onto a small target, allows various biological and therapeutic effects – for example the thermo-ablation of tissues using high-intensity FUS.[22, 77] Furthermore, both the imaging and therapeutic potential of US can be expanded massively in combination with microbubbles as well as other ultrasound responsive materials (**Figure 2K**). The acoustic backscattering of microbubbles allows their use as US contrast agents and has even permitted the resolution limit, sub-millimeter at best, of US imaging to be overcome.[78, 79] As well as providing beneficial imaging properties, the oscillation of microbubbles and other gas vesicles in the presence of FUS (known as cavitation) can be exploited for a variety of promising therapeutic applications. One interesting nanotheranostic study demonstrated low-frequency FUS could convert a unique class of genetically encodable, US imageable, gas vesicles (GV) into cavitating microbubbles, unleashing potent mechanical effects. Tumor-targeted microbes could be engineered to be expressed the GV allowing them to produce local mechanical damage and release drug cargo within tumors on command with FUS, whilst being non-invasively trackable using US.[80]

Micro/nano-bubbles can also be utilized to enhance drug delivery. Most notably, the stable cavitation of microbubbles under FUS within the vasculature induces mechanical forces on the blood–brain barrier (BBB) that transiently increase its permeability for drug delivery.[81, 82] In the context of nanotheranostics, FUS can allow the delivery of nanoparticles across the BBB for both imaging and therapy. Liposomes containing imaging and therapeutic agents with diameters ranging between 55 – 200 nm have been successfully delivered across the BBB using FUS in combination with microbubbles. [83, 84] In addition to increasing delivery across the BBB, US can be used to enhance the EPR effect too, by improving extravasation of nanomedicines to tumor sites.[85] A key study demonstrated that with consecutive injection of fluorescently-tagged liposomes and microbubbles US allowed improved delivery of nanoparticles to mouse tumors. The liposomes were imaged with both fluorescence molecular tomography and fluorescence

microscopy, which clearly showed increased uptake in both 'high EPR' and 'low EPR' tumor models.[86]

1.11 Focused ultrasound nanotheranostics

In the context of US-enhanced drug delivery, the imaging and therapy aspects are often two distinct platforms. However, a prominent area of US-based nanotheranostics is the development of single drug delivery platforms that are both imageable and triggerable using US. At higher ultrasound intensities, bubbles oscillate with increasingly large amplitudes and then burst, which can disrupt nearby cells or tissue (**Figure 2L**). Hence, by incorporating drugs into microbubbles and other ultrasound responsive particles, US can be used to trigger drug release via particle bursting, as well as increasing cellular entry of the therapeutic cargo.[78] A prominent example reported cancer immunotherapy based on US-activation of the cGAS-STING pathway. Nanocomplexes containing 2′3′-cyclic guanosine monophosphate-adenosine monophosphate (cGAMP) – capable of activating cGAS-STING – were conjugated onto microbubbles targeting antigen-presenting cells *via* anti-CD11b antibodies. Local delivery of the microbubbles coupled with FUS showed prominent STING-dependent inhibition of tumor growth, whilst also potentiating anti-PD-1 checkpoint inhibitor immunotherapy in both localized and metastatic murine cancer models.[87] Importantly, the presence of microbubbles at the tumor site, as well as their destruction after US sonoporation, could be observed non-invasively using contrast-mode US imaging. Aside from microbubbles, a variety of other ultrasound-responsive micro/nanocarriers have been reported,[88] which can offer potential benefits as nanotheranostics. For example, one study reported the use of nanobubbles produced by Halobacterium NRC-1 as a platform for image-guided ultrasonic gene delivery.[89] Finally, US-based nanotheranostics may also allow repeated-triggering of drug release. One study reported an injectable nanotheranostic system for local anesthetic based on micron-sized liposomes encapsulating tetrodotoxin, an anesthetic, and a sonosensitizer protoporphyrin IX (PPIX) in the lipid membrane – allowing ultrasonic-triggered release of the anaesthetic.[90] The liposomes were visualized with ultrasound allowing the authors to better target the injection to be in proximity with the sciatic nerve of rats. The nerve blocking activity was then demonstrated by an increase in time a rat would leave its hind paw on a hotplate. Crucially, after an initial nerve block following administration, it was shown that nerve blocking could be 're-activated' two subsequent times by ultrasound application.

	THERAPEUTIC MODALITY	IMAGING AGENT	THERAPEUTIC AGENT	STAGE
MAGNETIC RESONANCE IMAGING	nanomedicine	Gd^{3+}, Mn^{2+}, IONP	small molecule	pre-Clinical and Clinical
	thermal ablation	IONP	IONP (magnetic) PTA (photothermal)	pre-Clinical & Clinical
	radiation therapy	Gd^{3+}, Gd_2O_3, IONP	Au, Bi, Gd-complexes	pre-Clinical & Clinical
	HIFU & nanomedicine	MRI contrast	HIFU triggering of nanomedicine	pre-Clinical
	Image-guided cell therapies	IONP (intracellular)	cellular therapies	Clinical
	Image-guided surgery	IONP	surgery	Clinical
NUCLEAR IMAGING	'companion' nanoparticle	^{64}Cu, ^{89}Zr, ... (PET imaging)	nanomedicine	pre-Clinical & Clinical
	radiation therapy	^{64}Cu, ^{89}Zr, … (PET imaging)	^{177}Lu, ^{90}Y, $^{186/188}Re$	pre-Clinical
	CRIT	^{64}Cu, ^{89}Zr, … (PET imaging)	porphyrins, chlorins	pre-Clinical
OPTICAL IMAGING	photodynamic therapy	Cy5.5, Cy7; PLNP	porphyrins, chlorins, nanomedicine	pre-Clinical
	image-guided surgery	Cy5.5, Cy7; PLNP; DCNP	surgery	pre-Clinical & Clinical
	nanomedicine	endogenous, AuNP, CNT	small/macro-molecules	pre-Clinical
ULTRASOUND	enhanced delivery	vesicles	small/macro-molecules, nanomedicine	pre-Clinical
	triggered drug release	vesicles	drug-loaded vesicles	pre-Clinical and Clinical

Supplementary Table 1 | Preclinical and clinical nanotheranostics. Most relevant nanotheranostics organized by imaging and therapeutic modality.

SUPPLEMENTARY REFERENCES

1. Wahsner, J.; Gale, E. M.; Rodríguez-Rodríguez, A.; Caravan, P., Chemistry of MRI contrast agents: current challenges and new frontiers. *Chemical reviews* **2018,** *119* (2), 957-1057.

2. Brito, B.; Price, T. W.; Gallo, J.; Bañobre-López, M.; Stasiuk, G. J., Smart magnetic resonance imaging-based theranostics for cancer. *Theranostics* **2021,** *11* (18), 8706.

3. Gunasangkaran, G.; Ravi, A. K.; Arumugam, V. A.; Muthukrishnan, S., Preparation, Characterization, and Anticancer Efficacy of Chitosan, Chitosan Encapsulated Piperine and Probiotics (Lactobacillus plantarum (MTCC-1407), and Lactobacillus rhamnosus (MTCC-1423) Nanoparticles. *BioNanoScience* **2022,** *12* (2), 527-539.

4. Demirel, G. B.; Bayrak, Ş., Ultrasound/redox/pH-responsive hybrid nanoparticles for triple-triggered drug delivery. *Journal of Drug Delivery Science and Technology* **2022,** *71*, 103267.

5. Veselov, V. V.; Nosyrev, A. E.; Jicsinszky, L.; Alyautdin, R. N.; Cravotto, G., Targeted Delivery Methods for Anticancer Drugs. *Cancers* **2022,** *14* (3), 622.

6. Vinh, N. Q.; Naka, S.; Cabral, H.; Murayama, H.; Kaida, S.; Kataoka, K.; Morikawa, S.; Tani, T., MRI-detectable polymeric micelles incorporating platinum anticancer drugs enhance survival in an advanced hepatocellular carcinoma model. *International Journal of Nanomedicine* **2015,** *10*, 4137.

7. Hao, G.; Xu, Z. P.; Li, L., Manipulating extracellular tumour pH: an effective target for cancer therapy. *RSC Advances* **2018,** *8* (39), 22182-22192.

8. Benyettou, F.; Das, G.; Nair, A. R.; Prakasam, T.; Shinde, D. B.; Sharma, S. K.; Whelan, J.; Lalatonne, Y.; Traboulsi, H.; Pasricha, R., Covalent organic framework embedded with magnetic nanoparticles for MRI and chemo-thermotherapy. *Journal of the American Chemical Society* **2020,** *142* (44), 18782-18794.

9. Shen, Z.; Chen, T.; Ma, X.; Ren, W.; Zhou, Z.; Zhu, G.; Zhang, A.; Liu, Y.; Song, J.; Li, Z., Multifunctional theranostic nanoparticles based on exceedingly small magnetic iron oxide nanoparticles for T 1-weighted magnetic resonance imaging and chemotherapy. *ACS nano* **2017,** *11* (11), 10992-11004.

10. Lee, M. H.; Kim, E.-J.; Lee, H.; Kim, H. M.; Chang, M. J.; Park, S. Y.; Hong, K. S.; Kim, J. S.; Sessler, J. L., Liposomal texaphyrin theranostics for metastatic liver cancer. *Journal of the American Chemical Society* **2016,** *138* (50), 16380-16387.

11. Liu, Y.; Chi, S.; Cao, Y.; Liu, Z., Glutathione-Responsive Biodegradable Core–Shell Nanoparticles That Self-Generate H2O2 and Deliver Doxorubicin for Chemo–Chemodynamic Therapy. *ACS Applied Nano Materials* **2022,** *5* (2), 2592-2602.

12. Alizadeh, A. A.; Aranda, V.; Bardelli, A.; Blanpain, C.; Bock, C.; Borowski, C.; Caldas, C.; Califano, A.; Doherty, M.; Elsner, M.; Esteller, M.; Fitzgerald, R.; Korbel, J. O.; Lichter,

P.; Mason, C. E.; Navin, N.; Pe'er, D.; Polyak, K.; Roberts, C. W. M.; Siu, L.; Snyder, A.; Stower, H.; Swanton, C.; Verhaak, R. G. W.; Zenklusen, J. C.; Zuber, J.; Zucman-Rossi, J., Toward understanding and exploiting tumor heterogeneity. *Nature Medicine* **2015,** *21* (8), 846-853.

13. Reddy, L. H.; Arias, J. L.; Nicolas, J.; Couvreur, P., Magnetic nanoparticles: design and characterization, toxicity and biocompatibility, pharmaceutical and biomedical applications. *Chem Rev* **2012,** *112* (11), 5818-78.

14. Soleymani, M.; Khalighfard, S.; Khodayari, S.; Khodayari, H.; Kalhori, M. R.; Hadjighassem, M. R.; Shaterabadi, Z.; Alizadeh, A. M., Effects of multiple injections on the efficacy and cytotoxicity of folate-targeted magnetite nanoparticles as theranostic agents for MRI detection and magnetic hyperthermia therapy of tumor cells. *Scientific reports* **2020,** *10* (1), 1-14.

15. Cho, M.; Cervadoro, A.; Ramirez, M. R.; Stigliano, C.; Brazdeikis, A.; Colvin, V. L.; Civera, P.; Key, J.; Decuzzi, P., Assembly of Iron Oxide Nanocubes for Enhanced Cancer Hyperthermia and Magnetic Resonance Imaging. *Nanomaterials (Basel)* **2017,** *7* (4).

16. Du, Y.; Liu, X.; Liang, Q.; Liang, X.-J.; Tian, J., Optimization and Design of Magnetic Ferrite Nanoparticles with Uniform Tumor Distribution for Highly Sensitive MRI/MPI Performance and Improved Magnetic Hyperthermia Therapy. *Nano Letters* **2019,** *19* (6), 3618-3626.

17. Mai, B. T.; Balakrishnan, P. B.; Barthel, M. J.; Piccardi, F.; Niculaes, D.; Marinaro, F.; Fernandes, S.; Curcio, A.; Kakwere, H.; Autret, G.; Cingolani, R.; Gazeau, F.; Pellegrino, T., Thermoresponsive Iron Oxide Nanocubes for an Effective Clinical Translation of Magnetic Hyperthermia and Heat-Mediated Chemotherapy. *ACS Appl Mater Interfaces* **2019,** *11* (6), 5727-5739.

18. Li, X.; Lovell, J. F.; Yoon, J.; Chen, X., Clinical development and potential of photothermal and photodynamic therapies for cancer. *Nature Reviews Clinical Oncology* **2020,** *17* (11), 657-674.

19. DuRoss, A. N.; Phan, J.; Lazar, A. J.; Walker, J. M.; Guimaraes, A. R.; Baas, C.; Krishnan, S.; Thomas Jr, C. R.; Sun, C.; Bagley, A. F., Radiotherapy reimagined: Integrating nanomedicines into radiotherapy clinical trials. *WIREs Nanomedicine and Nanobiotechnology n/a* (n/a), e1867.

20. Ma, M.; Huang, Y.; Chen, H.; Jia, X.; Wang, S.; Wang, Z.; Shi, J., Bi2S3-embedded mesoporous silica nanoparticles for efficient drug delivery and interstitial radiotherapy sensitization. *Biomaterials* **2015,** *37*, 447-455.

21. Wu, C.; Cai, R.; Zhao, T.; Wu, L.; Zhang, L.; Jin, J.; Xu, L.; Li, P.; Li, T.; Zhang, M., Hyaluronic acid-functionalized gadolinium oxide nanoparticles for magnetic resonance imaging-guided radiotherapy of tumors. *Nanoscale research letters* **2020,** *15* (1), 1-12.

22. Meng, Y.; Hynynen, K.; Lipsman, N., Applications of focused ultrasound in the brain: from thermoablation to drug delivery. *Nat Rev Neurol* **2021,** *17* (1), 7-22.

23. Cabras, P.; Auloge, P.; Bing, F.; Rao, P. P.; Hoarau, S.; Dumont, E.; Durand, A.; Maurin, B.; Wach, B.; Cuvillon, L.; Breton, E.; Gangi, A.; Vappou, J., A new versatile MR-guided high-intensity focused ultrasound (HIFU) device for the treatment of musculoskeletal tumors. *Scientific Reports* **2022,** *12* (1), 9095.

24. Thébault, C. J.; Ramniceanu, G.; Boumati, S.; Michel, A.; Seguin, J.; Larrat, B.; Mignet, N.; Ménager, C.; Doan, B.-T., Theranostic MRI liposomes for magnetic targeting and ultrasound triggered release of the antivascular CA4P. *Journal of Controlled Release* **2020,** *322*, 137-148.

25. Centelles, M. N.; Wright, M.; So, P.-W.; Amrahli, M.; Xu, X. Y.; Stebbing, J.; Miller, A. D.; Gedroyc, W.; Thanou, M., Image-guided thermosensitive liposomes for focused ultrasound drug delivery: Using NIRF-labelled lipids and topotecan to visualise the effects of hyperthermia in tumours. *Journal of Controlled Release* **2018,** *280*, 87-98.

26. Pellico, J.; Gawne, P. J.; R, T. M. d. R., Radiolabelling of nanomaterials for medical imaging and therapy. *Chem Soc Rev* **2021,** *50* (5), 3355-3423.

27. Perez-Medina, C.; Teunissen, A. J. P.; Kluza, E.; Mulder, W. J. M.; van der Meel, R., Nuclear imaging approaches facilitating nanomedicine translation. *Adv Drug Deliv Rev* **2020,** *154-155*, 123-141.

28. Tang, J.; Baxter, S.; Menon, A.; Alaarg, A.; Sanchez-Gaytan, B. L.; Fay, F.; Zhao, Y.; Ouimet, M.; Braza, M. S.; Longo, V. A.; Abdel-Atti, D.; Duivenvoorden, R.; Calcagno, C.; Storm, G.; Tsimikas, S.; Moore, K. J.; Swirski, F. K.; Nahrendorf, M.; Fisher, E. A.; Perez-Medina, C.; Fayad, Z. A.; Reiner, T.; Mulder, W. J., Immune cell screening of a nanoparticle library improves atherosclerosis therapy. *Proc Natl Acad Sci U S A* **2016,** *113* (44), E6731-E6740.

29. Zhang, X.; Cherry, S. R.; Xie, Z.; Shi, H.; Badawi, R. D.; Qi, J., Subsecond total-body imaging using ultrasensitive positron emission tomography. *Proc Natl Acad Sci U S A* **2020,** *117* (5), 2265-2267.

30. Binderup, T.; Duivenvoorden, R.; Fay, F.; van Leent, M. M. T.; Malkus, J.; Baxter, S.; Ishino, S.; Zhao, Y.; Sanchez-Gaytan, B.; Teunissen, A. J. P.; Frederico, Y. C. A.; Tang, J.; Carlucci, G.; Lyashchenko, S.; Calcagno, C.; Karakatsanis, N.; Soultanidis, G.; Senders, M. L.; Robson, P. M.; Mani, V.; Ramachandran, S.; Lobatto, M. E.; Hutten, B. A.; Granada, J. F.; Reiner, T.; Swirski, F. K.; Nahrendorf, M.; Kjaer, A.; Fisher, E. A.; Fayad, Z. A.; Perez-Medina, C.; Mulder, W. J. M., Imaging-assisted nanoimmunotherapy for atherosclerosis in multiple species. *Sci Transl Med* **2019,** *11* (506).

31. Harrington, K. J.; Mohammadtaghi, S.; Uster, P. S.; Glass, D.; Peters, A. M.; Vile, R. G.; Stewart, J. S., Effective targeting of solid tumors in patients with locally advanced cancers by radiolabeled pegylated liposomes. *Clin Cancer Res* **2001,** *7* (2), 243-54.

32. Nichols, J. W.; Bae, Y. H., EPR: Evidence and fallacy. *J Control Release* **2014,** *190*, 451-64.

33. Prabhakar, U.; Maeda, H.; Jain, R. K.; Sevick-Muraca, E. M.; Zamboni, W.; Farokhzad, O. C.; Barry, S. T.; Gabizon, A.; Grodzinski, P.; Blakey, D. C., Challenges and key considerations of the enhanced permeability and retention effect for nanomedicine drug delivery in oncology. *Cancer Res* **2013,** *73* (8), 2412-7.

34. Lammers, T.; Rizzo, L. Y.; Storm, G.; Kiessling, F., Personalized nanomedicine. *Clin Cancer Res* **2012,** *18* (18), 4889-94.

35. Edmonds, S.; Volpe, A.; Shmeeda, H.; Parente-Pereira, A. C.; Radia, R.; Baguna-Torres, J.; Szanda, I.; Severin, G. W.; Livieratos, L.; Blower, P. J.; Maher, J.; Fruhwirth, G. O.; Gabizon, A.; R, T. M. d. R., Exploiting the Metal-Chelating Properties of the Drug Cargo for In Vivo Positron Emission Tomography Imaging of Liposomal Nanomedicines. *ACS Nano* **2016,** *10* (11), 10294-10307.

36. Gawne, P. J.; Clarke, F.; Turjeman, K.; Cope, A. P.; Long, N. J.; Barenholz, Y.; Terry, S. Y. A.; de Rosales, R. T. M., PET Imaging of Liposomal Glucocorticoids using (89)Zr-oxine: Theranostic Applications in Inflammatory Arthritis. *Theranostics* **2020,** *10* (9), 3867-3879.

37. Lee, H.; Gaddy, D.; Ventura, M.; Bernards, N.; de Souza, R.; Kirpotin, D.; Wickham, T.; Fitzgerald, J.; Zheng, J.; Hendriks, B. S., Companion Diagnostic (64)Cu-Liposome Positron

Emission Tomography Enables Characterization of Drug Delivery to Tumors and Predicts Response to Cancer Nanomedicines. *Theranostics* **2018,** *8* (9), 2300-2312.

38. Perez-Medina, C.; Abdel-Atti, D.; Tang, J.; Zhao, Y.; Fayad, Z. A.; Lewis, J. S.; Mulder, W. J. M.; Reiner, T., Nanoreporter PET predicts the efficacy of anti-cancer nanotherapy. *Nat Commun* **2016,** *7*, 11838.

39. Herrero Alvarez, N.; Bauer, D.; Hernandez-Gil, J.; Lewis, J. S., Recent Advances in Radiometals for Combined Imaging and Therapy in Cancer. *ChemMedChem* **2021,** *16* (19), 2909-2941.

40. Ferreira, C. A.; Goel, S.; Ehlerding, E. B.; Rosenkrans, Z. T.; Jiang, D.; Sun, T.; Aluicio-Sarduy, E.; Engle, J. W.; Ni, D.; Cai, W., Ultrasmall Porous Silica Nanoparticles with Enhanced Pharmacokinetics for Cancer Theranostics. *Nano Lett* **2021,** *21* (11), 4692-4699.

41. Kotagiri, N.; Sudlow, G. P.; Akers, W. J.; Achilefu, S., Breaking the depth dependency of phototherapy with Cerenkov radiation and low-radiance-responsive nanophotosensitizers. *Nat Nanotechnol* **2015,** *10* (4), 370-9.

42. Tang, R.; Zheleznyak, A.; Mixdorf, M.; Ghai, A.; Prior, J.; Black, K. C. L.; Shokeen, M.; Reed, N.; Biswas, P.; Achilefu, S., Osteotropic Radiolabeled Nanophotosensitizer for Imaging and Treating Multiple Myeloma. *ACS Nano* **2020,** *14* (4), 4255-4264.

43. Kamkaew, A.; Cheng, L.; Goel, S.; Valdovinos, H. F.; Barnhart, T. E.; Liu, Z.; Cai, W., Cerenkov Radiation Induced Photodynamic Therapy Using Chlorin e6-Loaded Hollow Mesoporous Silica Nanoparticles. *ACS Appl Mater Interfaces* **2016,** *8* (40), 26630-26637.

44. Ni, D.; Ferreira, C. A.; Barnhart, T. E.; Quach, V.; Yu, B.; Jiang, D.; Wei, W.; Liu, H.; Engle, J. W.; Hu, P.; Cai, W., Magnetic Targeting of Nanotheranostics Enhances Cerenkov Radiation-Induced Photodynamic Therapy. *J Am Chem Soc* **2018,** *140* (44), 14971-14979.

45. Yu, B.; Ni, D.; Rosenkrans, Z. T.; Barnhart, T. E.; Wei, H.; Ferreira, C. A.; Lan, X.; Engle, J. W.; He, Q.; Yu, F.; Cai, W., A "Missile-Detonation" Strategy to Precisely Supply and Efficiently Amplify Cerenkov Radiation Energy for Cancer Theranostics. *Adv Mater* **2019,** *31* (52), e1904894.

46. Debbage, P.; Jaschke, W., Molecular imaging with nanoparticles: giant roles for dwarf actors. *Histochemistry and cell biology* **2008,** *130* (5), 845-875.

47. Park, K.; Lee, S.; Kang, E.; Kim, K.; Choi, K.; Kwon, I. C., New generation of multifunctional nanoparticles for cancer imaging and therapy. *Advanced functional materials* **2009,** *19* (10), 1553-1566.

48. Yang, G.; Yang, D.; Yang, P.; Lv, R.; Li, C.; Zhong, C.; He, F.; Gai, S.; Lin, J., A Single 808 nm Near-Infrared Light-Mediated Multiple Imaging and Photodynamic Therapy Based on Titania Coupled Upconversion Nanoparticles. *Chemistry of Materials* **2015,** *27* (23), 7957-7968.

49. Sun, S.-K.; Wang, H.-F.; Yan, X.-P., Engineering Persistent Luminescence Nanoparticles for Biological Applications: From Biosensing/Bioimaging to Theranostics. *Accounts of Chemical Research* **2018,** *51* (5), 1131-1143.

50. Wang, J.; Ma, Q.; Hu, X.-X.; Liu, H.; Zheng, W.; Chen, X.; Yuan, Q.; Tan, W., Autofluorescence-free targeted tumor imaging based on luminous nanoparticles with composition-dependent size and persistent luminescence. *ACS nano* **2017,** *11* (8), 8010-8017.

51. Maldiney, T.; Bessière, A.; Seguin, J.; Teston, E.; Sharma, S. K.; Viana, B.; Bos, A. J.; Dorenbos, P.; Bessodes, M.; Gourier, D., The in vivo activation of persistent nanophosphors for optical imaging of vascularization, tumours and grafted cells. *Nature materials* **2014,** *13* (4), 418-426.

52. Zheng, B.; Bai, Y.; Chen, H.; Pan, H.; Ji, W.; Gong, X.; Wu, X.; Wang, H.; Chang, J., Near-infrared light-excited upconverting persistent nanophosphors in vivo for imaging-guided cell therapy. *ACS applied materials & interfaces* **2018,** *10* (23), 19514-19522.

53. Xue, Z.; Li, X.; Li, Y.; Jiang, M.; Ren, G.; Liu, H.; Zeng, S.; Hao, J., A 980 nm laser-activated upconverted persistent probe for NIR-to-NIR rechargeable in vivo bioimaging. *Nanoscale* **2017,** *9* (21), 7276-7283.

54. Zheng, S.; Shi, J.; Fu, X.; Wang, C.; Sun, X.; Chen, C.; Zhuang, Y.; Zou, X.; Li, Y.; Zhang, H., X-ray recharged long afterglow luminescent nanoparticles MgGeO 3: Mn 2+, Yb 3+, Li+ in the first and second biological windows for long-term bioimaging. *Nanoscale* **2020,** *12* (26), 14037-14046.

55. Liu, N.; Shi, J.; Wang, Q.; Guo, J.; Hou, Z.; Su, X.; Zhang, H.; Sun, X., In Vivo Repeatedly Activated Persistent Luminescence Nanoparticles by Radiopharmaceuticals for Long-Lasting Tumor Optical Imaging. *Small* **2020,** *16* (26), 2001494.

56. Chen, L.-J.; Yang, C.-X.; Yan, X.-P., Liposome-Coated Persistent Luminescence Nanoparticles as Luminescence Trackable Drug Carrier for Chemotherapy. *Analytical Chemistry* **2017,** *89* (13), 6936-6939.

57. Zhao, X.; Zhao, K.-C.; Chen, L.-J.; Liu, Y.-S.; Liu, J.-L.; Yan, X.-P., A pH reversibly activatable NIR photothermal/photodynamic-in-one agent integrated with renewable nanoimplants for image-guided precision phototherapy. *Chemical science* **2021,** *12* (1), 442-452.

58. Hu, F.; Xu, S.; Liu, B., Photosensitizers with Aggregation-Induced Emission: Materials and Biomedical Applications. *Advanced Materials* **2018,** *30* (45), 1801350.

59. Cao, J.; Chi, J.; Xia, J.; Zhang, Y.; Han, S.; Sun, Y., Iodinated Cyanine Dyes for Fast Near-Infrared-Guided Deep Tissue Synergistic Phototherapy. *ACS Applied Materials & Interfaces* **2019,** *11* (29), 25720-25729.

60. Mieog, J. S. D.; Achterberg, F. B.; Zlitni, A.; Hutteman, M.; Burggraaf, J.; Swijnenburg, R.-J.; Gioux, S.; Vahrmeijer, A. L., Fundamentals and developments in fluorescence-guided cancer surgery. *Nature Reviews Clinical Oncology* **2022,** *19* (1), 9-22.

61. Xi, L.; Jiang, H., Image-guided surgery using multimodality strategy and molecular probes. *Wiley Interdisciplinary Reviews: Nanomedicine and Nanobiotechnology* **2016,** *8* (1), 46-60.

62. Wang, P.; Fan, Y.; Lu, L.; Liu, L.; Fan, L.; Zhao, M.; Xie, Y.; Xu, C.; Zhang, F., NIR-II nanoprobes in-vivo assembly to improve image-guided surgery for metastatic ovarian cancer. *Nature Communications* **2018,** *9* (1), 2898.

63. Shi, X.; Gao, K.; Xiong, S.; Gao, R., Multifunctional Transferrin Encapsulated GdF3 Nanoparticles for Sentinel Lymph Node and Tumor Imaging. *Bioconjugate Chemistry* **2020,** *31* (11), 2576-2584.

64. van der Zaag, E. S.; Bouma, W. H.; Tanis, P. J.; Ubbink, D. T.; Bemelman, W. A.; Buskens, C. J., Systematic Review of Sentinel Lymph Node Mapping Procedure in Colorectal Cancer. *Annals of Surgical Oncology* **2012,** *19* (11), 3449-3459.

65. Dell'Orto, F.; Laven, P.; Delle Marchette, M.; Lambrechts, S.; Kruitwagen, R.; Buda, A., Feasibility of sentinel lymph node mapping of the ovary: a systematic review. *International Journal of Gynecologic Cancer* **2019,** *29* (7), 1209-1215.

66. Li, J.; Chen, X.; Qi, M.; Li, Y., Sentinel lymph node biopsy mapped with methylene blue dye alone in patients with breast cancer: A systematic review and meta-analysis. *PLOS ONE* **2018,** *13* (9), e0204364.

67. Yin, L.; Sun, H.; Zhao, M.; Wang, A.; Qiu, S.; Gao, Y.; Ding, J.; Ji, S.-J.; Shi, H.; Gao, M., Rational Design and Synthesis of a Metalloproteinase-Activatable Probe for Dual-Modality Imaging of Metastatic Lymph Nodes in Vivo. *The Journal of Organic Chemistry* **2019,** *84* (10), 6126-6133.

68. Shi, H.; Yan, R.; Wu, L.; Sun, Y.; Liu, S.; Zhou, Z.; He, J.; Ye, D., Tumor-targeting CuS nanoparticles for multimodal imaging and guided photothermal therapy of lymph node metastasis. *Acta Biomaterialia* **2018,** *72*, 256-265.

69. de Vries, M.; Jager, P. L.; Suurmeijer, A. J. H.; Plukker, J. T. M.; van Ginkel, R. J.; Hoekstra, H. J., [Sentinel lymph node biopsy for melanoma: prognostic value and disadvantages in 300 patients]. *Ned Tijdschr Geneeskd* **2005,** *149* (33), 1845-1851.

70. Rousseau, C.; Classe, J. M.; Campion, L.; Curtet, C.; Dravet, F.; Pioud, R.; Sagan, C.; Bridji, B.; Resche, I., The impact of nonvisualization of sentinel nodes on lymphoscintigraphy in breast cancer. *Ann Surg Oncol* **2005,** *12* (7), 533-8.

71. Lin, L.; Wang, L. V., The emerging role of photoacoustic imaging in clinical oncology. *Nature Reviews Clinical Oncology* **2022,** *19* (6), 365-384.

72. Kim, J.; Kim, J. Y.; Jeon, S.; Baik, J. W.; Cho, S. H.; Kim, C., Super-resolution localization photoacoustic microscopy using intrinsic red blood cells as contrast absorbers. *Light: Science & Applications* **2019,** *8* (1), 103.

73. Stoffels, I.; Morscher, S.; Helfrich, I.; Hillen, U.; Leyh, J.; Burton, N. C.; Sardella, T. C.; Claussen, J.; Poeppel, T. D.; Bachmann, H. S.; Roesch, A.; Griewank, K.; Schadendorf, D.; Gunzer, M.; Klode, J., Metastatic status of sentinel lymph nodes in melanoma determined noninvasively with multispectral optoacoustic imaging. *Sci Transl Med* **2015,** *7* (317), 317ra199.

74. Han, S.; Lee, D.; Kim, S.; Kim, H. H.; Jeong, S.; Kim, J., Contrast Agents for Photoacoustic Imaging: A Review Focusing on the Wavelength Range. *Biosensors (Basel)* **2022,** *12* (8).

75. Ferrauto, G.; Carniato, F.; Di Gregorio, E.; Botta, M.; Tei, L., Photoacoustic ratiometric assessment of mitoxantrone release from theranostic ICG-conjugated mesoporous silica nanoparticles. *Nanoscale* **2019,** *11* (39), 18031-18036.

76. Fan, Z.; Wang, Y.; Li, L.; Zeng, F.; Shang, Q.; Liao, Y.; Liang, C.; Nie, L., Tumor-Homing and Immune-Reprogramming Cellular Nanovesicles for Photoacoustic Imaging-Guided Phototriggered Precise Chemoimmunotherapy. *ACS Nano* **2022,** *16* (10), 16177-16190.

77. Ebbini, E. S.; Ter Haar, G., Ultrasound-guided therapeutic focused ultrasound: Current status and future directions. *International Journal of Hyperthermia* **2015,** *31* (2), 77-89.

78. Wang, Y.; Kohane, D. S., External triggering and triggered targeting strategies for drug delivery. *Nature Reviews Materials* **2017,** *2* (6), 17020.

79. Errico, C.; Pierre, J.; Pezet, S.; Desailly, Y.; Lenkei, Z.; Couture, O.; Tanter, M., Ultrafast ultrasound localization microscopy for deep super-resolution vascular imaging. *Nature* **2015,** *527* (7579), 499-502.

80. Bar-Zion, A.; Nourmahnad, A.; Mittelstein, D. R.; Shivaei, S.; Yoo, S.; Buss, M. T.; Hurt, R. C.; Malounda, D.; Abedi, M. H.; Lee-Gosselin, A.; Swift, M. B.; Maresca, D.; Shapiro, M. G., Acoustically triggered mechanotherapy using genetically encoded gas vesicles. *Nat Nanotechnol* **2021,** *16* (12), 1403-1412.

81. Hynynen, K.; McDannold, N.; Vykhodtseva, N.; Jolesz, F. A., Noninvasive MR imaging-guided focal opening of the blood-brain barrier in rabbits. *Radiology* **2001,** *220* (3), 640-6.

82. Terstappen, G. C.; Meyer, A. H.; Bell, R. D.; Zhang, W., Strategies for delivering therapeutics across the blood-brain barrier. *Nat Rev Drug Discov* **2021,** *20* (5), 362-383.

83. Morse, S. V.; Mishra, A.; Chan, T. G.; R, T. M. d. R.; Choi, J. J., Liposome delivery to the brain with rapid short-pulses of focused ultrasound and microbubbles. *J Control Release* **2022,** *341*, 605-615.

84. Morse, S. V.; Pouliopoulos, A. N.; Chan, T. G.; Copping, M. J.; Lin, J.; Long, N. J.; Choi, J. J., Rapid Short-pulse Ultrasound Delivers Drugs Uniformly across the Murine Blood-Brain Barrier with Negligible Disruption. *Radiology* **2019,** *291* (2), 459-466.

85. Duan, L.; Yang, L.; Jin, J.; Yang, F.; Liu, D.; Hu, K.; Wang, Q.; Yue, Y.; Gu, N., Micro/nano-bubble-assisted ultrasound to enhance the EPR effect and potential theranostic applications. *Theranostics* **2020,** *10* (2), 462-483.

86. Theek, B.; Baues, M.; Ojha, T.; Mockel, D.; Veettil, S. K.; Steitz, J.; van Bloois, L.; Storm, G.; Kiessling, F.; Lammers, T., Sonoporation enhances liposome accumulation and penetration in tumors with low EPR. *J Control Release* **2016,** *231*, 77-85.

87. Li, X.; Khorsandi, S.; Wang, Y.; Santelli, J.; Huntoon, K.; Nguyen, N.; Yang, M.; Lee, D.; Lu, Y.; Gao, R.; Kim, B. Y. S.; de Gracia Lux, C.; Mattrey, R. F.; Jiang, W.; Lux, J., Cancer immunotherapy based on image-guided STING activation by nucleotide nanocomplex-decorated ultrasound microbubbles. *Nat Nanotechnol* **2022,** *17* (8), 891-899.

88. Chandan, R.; Mehta, S.; Banerjee, R., Ultrasound-Responsive Carriers for Therapeutic Applications. *ACS Biomater Sci Eng* **2020,** *6* (9), 4731-4747.

89. Tayier, B.; Deng, Z.; Wang, Y.; Wang, W.; Mu, Y.; Yan, F., Biosynthetic nanobubbles for targeted gene delivery by focused ultrasound. *Nanoscale* **2019,** *11* (31), 14757-14768.

90. Rwei, A. Y.; Paris, J. L.; Wang, B.; Wang, W.; Axon, C. D.; Vallet-Regi, M.; Langer, R.; Kohane, D. S., Ultrasound-triggered local anaesthesia. *Nat Biomed Eng* **2017,** *1*, 644-653.